Environ Sci Pollut Res (2012) 19:2983–2993
DOI 10.1007/s11356-012-0809-0

RESEARCH ARTICLE

Biosorption of Cr(VI) by free and immobilized *Pediastrum boryanum* biomass: equilibrium, kinetic, and thermodynamic studies

T. Baykal Ozer · I. Acıkgoz Erkaya · Abel U. Udoh · D. Yalcın Duygu · Aydın Akbulut · Gulay Bayramoglu · M. Yakup Arica

Received: 27 July 2011 / Accepted: 2 February 2012 / Published online: 29 February 2012

Abstract
Background and purpose The biosorption of Cr(VI) from aqueous solution has been studied using free and immobilized *Pediastrum boryanum* cells in a batch system. The algal cells were immobilized in alginate and alginate–gelatin beads via entrapment, and their algal cell free counterparts were used as control systems during biosorption studies of Cr(VI).
Methods The changes in the functional groups of the biosorbents formulations were confirmed by Fourier transform infrared spectra. The effect of pH, equilibrium time, initial concentration of metal ions, and temperature on the biosorption of Cr(VI) ion was investigated.
Results The maximum Cr(VI) biosorption capacities were found to be 17.3, 6.73, 14.0, 23.8, and 29.6 mg/g for the free algal cells, and alginate, alginate–gelatin, alginate–cells, and alginate–gelatin–cells at pH 2.0, which are corresponding to an initial Cr(VI) concentration of 400 mg/L. The biosorption of Cr(VI) on all the tested biosorbents (*P. boryanum* cells, alginate, alginate–gelatin, and alginate–cells, alginate–gelatin–cells) followed Langmuir adsorption isotherm model.
Conclusion The thermodynamic studies indicated that the biosorption process was spontaneous and endothermic in nature under studied conditions. For all the tested biosorbents, biosorption kinetic was best described by the pseudo-second-order model.

Keywords Cr(VI) · Alginate · Gelatin · *Pediastrum boryanum* · Immobilization · Biosorption

Responsible editor: Elena Maestri

T. B. Ozer
Department of Biology, Faculty of Arts and Science,
Ahi Evran University,
Kırsehir, Turkey

I. A. Erkaya · A. U. Udoh · D. Y. Duygu
Department of Biology Education, Faculty of Education,
Gazi University,
06500 Teknikokullar,
Ankara, Turkey

A. Akbulut (✉) · M. Y. Arica
Department of Biology, Faculty of Science, Gazi University,
06500 Teknikokullar,
Ankara, Turkey
e-mail: akbuluta@gazi.edu.tr

G. Bayramoglu (✉) · M. Y. Arica
Biochemical Processing and Biomaterial Research Laboratory,
Faculty of Sciences, Gazi University,
06500 Teknikokullar,
Ankara, Turkey
e-mail: g_bayramoglu@hotmail.com

1 Introduction

At least 20 metals are classified as toxic, and half of these are emitted into the environment in quantities that pose risks to human health. Among them, chromium is one of the most hazardous metals entering surface waters from the effluent of textile, tannery, electroplating, mining, and metal cleaning industries, and nuclear power plants (Gadd 1993; Arica et al. 2005; Sari et al. 2007). Toxicity of Cr(VI) is due to the negatively charged chromate (CrO_4^{-2}) and dichromate ($Cr_2O_7^{-2}$) anion complexes that easily pass through cellular membranes by means of sulfate ionic channels and then undergo immediate reduction reactions leading to the formation of various harmful reactive intermediates (Kuyucak and Volesky 1990). Hexavalent chromium anions are genotoxic and carcinogens. According to some researchers, the damage

is caused by hydroxyl radicals, produced during reoxidation of pentavalent chromium by hydrogen peroxide molecules present in the cell (Bajpai et al. 2004). The removal of heavy metal ions by biosorption using biological materials have been widely studied in the last decade due to its potential, particularly in wastewater treatment. Compared to some microbial biomasses such as fungi (Arica et al. 2004; Akar and Tunali 2006; Genc et al. 2003; Bayramoğlu et al. 2006), bacteria (Tuzen et al. 2007), and yeast (Cristani et al. 2011), heavy metal biosorption capacity of algae proved to be the highest because of the algal cell wall, which is composed of a fiber-like structure and an amorphous embedding matrix of various polysaccharides (Khani 2011; Bayramoglu and Arica 2009). In addition, algal cell surfaces carry various types of functional groups such as primary and secondary amino groups, sulfate, and carboxyl groups, which are responsible for the sequestration of heavy metals from aqueous medium (Silke and Volesky 1995; Yipmantin et al. 2011). The main attractions of biosorption are high selectivity and efficiency, cost effectiveness, good removal performance, possible regeneration at low cost and availability of known process equipment (Yang et al. 2011; Singha and Kumar 2011). The use of dead microbial biomass in biosorption is more advantageous for water treatment in that dead organisms are not affected by toxic wastes, they do not require a continuous supply of nutrients, and they can be regenerated and reused for many cycles (Bayramoglu and Arica 2008). However, the small size, low density, and organic leaching of algal biosorbents during the biosorption process hinder their applications (Bayramoglu and Arica 2009). Several synthetic (such as silica, polysulfone, polyurethanes, polyvinyl alcohol, and acrylate based polymers) and natural polymers (such as alginate, gelatin, agar, and cellulose derivative) have been used for the immobilization of microbial biomasses (Akar et al. 2009). Among them, alginate and gelatin as biodegradable support materials were used for immobilization of microbial cells (Bayramoglu and Arica 2009). Alginate is a linear polyurinate obtained from marine algae and contains variable amounts of D-manuronic and L-guluronic acid, which can be cross-linked using calcium ions. Gelatin is a partial degradation product of collagen; the amino acid residues are capable of interacting with metal ions, which contains primary and secondary amino groups, imidazole group, and the sulfhydryl group (Bajpai et al. 2004).

In this work, the removal of Cr(VI) ions from aqueous medium was studied using the free micro-algae cells (i.e. *Pediastrum boryanum*), and cells immobilized biosorbents. The algal cells were immobilized in the cross-linked alginate and alginate–gelatin composite matrices. Apart from the activity of algal biomass to interact with metal ions, the potential of the present work also arises from the fact that the amino acid residues of gelatin molecules have active groups that can also interact with Cr(VI) ions. According to our knowledge, there is no study reported with immobilized *P. boryanum* in alginate and alginate–gelatin systems. The functional groups, of all the tested biosorbents, were determined by Fourier transform infrared (FTIR). The effects of pH, adsorption time, and initial metal ion concentration were studied. The biosorption of Cr(VI) ions from aqueous solutions on all the tested biosorbents under different kinetic and equilibrium conditions are scrutinized in some details. The information gained from the work was expected to indicate whether the tested biosorbents may have the potential to be used for the removal and recovery of Cr(VI) ions from wastewaters.

2 Materials and methods

2.1 Microorganism and media

Individuals of *P. boryanum* species were collected from freshwaters during the field work. *P. boryanum* is a green alga. It is a non-motile coenobial (fixed number of cells) that inhabits freshwater environments. Algal cells were incubated for enrichment in nutrients medium (Allen medium, Bold–Wynee, soil extract, and urea Scenedesmus) at room temperature for 96 h. At the end of this incubation period, the samples of the microalgae were identified under the microscope as described previously (Wetzel and Likens 1991). Briefly, from the enriched mixed culture medium, a drop of the culture was transferred on a microscopic slide, and three drops of sterile culture medium were placed previously. The slide was placed under a microscope. With the help of a micropipette, the cells or group of cells to be isolated was taken and passed through the first, second, and third drops of sterile culture medium. After washing in the third drop, it was transferred into a dropping liquid nutrient medium and incubated at room temperature. The cell culture was incubated in nutrient medium at pH 6.8 and at 22±1°C for 96 h and was illuminated under light source with a distance of 20 cm from the top of the culture medium reactor. The lighting system was operated with 16:8 h of light–dark cycle. The intensity of light during the light period was 6,000 μmol cm^{-2} s^{-1}. In this system, sterile tubes connected to an aquarium engine that served both as ventilation and mixing systems were used. The wet weights of algal cells were derived from volume, assuming a cell-specific gravity of c.1. The volume of each cell was determined by approximating its shape to the nearest geometric configuration. The total biomass was calculated by multiplying the average number of cells with the average volume on each day during the growth of culture according to the method of Wetzel and Likens (1991). The micrograph of *P. boryanum* was obtained with a light microscope and presented in Fig. 1.

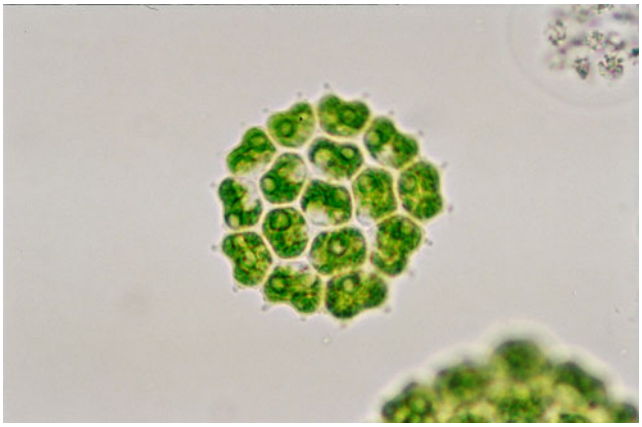

Fig. 1 The micrograph of *P. Boryanum* cells obtained with light microscope

2.2 Immobilization of microalga biomass into cross-linked alginate and alginate–gelatin

The immobilization of *P. boryanum* cells via entrapment into alginate beads was carried out as follows: Na alginate (2.0 g; from *Macrosytia pyrifera*, high viscosity, Sigma Chem. Co., USA) was dissolved in distilled water (50 ml), and it was then mixed with the algal suspension (50 mL, containing 1.0 g algal biomass). The mixture was introduced into a solution containing (0.1 M $CaCl_2$) with a burette, and the solution was stirred to prevent aggregation of the algal biomass entrapped in Ca alginate beads. The algal cells entrapped Ca alginate beads are called alginate–cell beads. The algal cell entrapped beads (~2 mm) were cured in this solution for 30 min and then washed twice with 200 ml sterile distilled water. It was then stored at 4°C until use in 5 mM $CaCl_2$ solution (Bayramoglu and Arica 2009).

The immobilization of *P. boryanum* biomass via entrapment into alginate–gelatin composite beads was carried out as described above except that gelatin (5.0 g) was added as a second natural polymer in the 2.0% Na alginate solution as described above. Briefly, after cross-linking alginate–gelatin composite beads with calcium ions, the composite Ca alginate–gelatin beads were treated with glutaraldehyde to form covalent linkage between gelatin units. In order to achieve this, the composite beads with entrapped algal cells (5.0 g) were equilibrated in phosphate buffer (20 mL, 50 mM, pH 7.0) for 6 h and transferred to the same buffer solution containing glutaraldehyde [50 ml, 0.5% (*v*/*v*)]. The cross-linking reaction was carried out at 25°C for 6.0 h while continuously stirring the medium. After the reaction period, the excess glutaraldehyde was removed by washing sequentially the composite beads with distilled water, acetic acid solution (0.1 M, 100 mL), and phosphate buffer. The resulting algal cell immobilized composite bead was referred as alginate–gelatin–cells beads. It was then stored at 4°C until use in 5 mM $CaCl_2$ solution.

2.3 Biosorption studies

Biosorption of Cr(VI) on the algal free cells, alginate, alginate–gelatin, alginate–cell, and alginate–gelatin–cell beads was investigated in batch biosorption-equilibrium experiments. The stock solutions of Cr(VI) anions (1.0 g/L) were prepared using the analytical grade dichromate salts in purified water. A range of metal ion concentration was prepared from stock solution. The effect of pH on the biosorption rate was investigated in the pH range of 1.0–8.0 (which was adjusted with HCl or NaOH at the beginning of the experiment and not controlled afterwards) at 25°C. The effect of temperature on the biosorption capacity of all the tested biosorbents was examined at four different temperatures (i.e., 15, 25, 35, and 45°C). The solution containing 100 mg/L of Cr (VI) anions (25 mL) and 0.1 g of biosorbents was stirred at 150 rpm. The effect of the initial metal ion concentration on the biosorption was studied at pH 2.0 for free cells, alginate, alginate–gelatin, alginate–cells, and alginate–gelatin–cell biosorbent systems as noted above except that the concentration of metal ions in the adsorption medium varied between 20 and 400 mg/L.

The concentration of remaining Cr(VI) in the biosorption medium was determined spectrophotometrically at 540 nm using a double beam UV/vis spectrophotometer (PG Instrument Ltd., Model T80+; PRC) after complexation with 1,5-diphenylcarbazide as described previously (Snell and Snell 1959). This colorimetric method can be used for the determination of Cr(VI) anions in natural and industrial water in the range of 100–1000 μg/L. In this method, before the determination of the total quantity of chromium Cr(VI) in the biosorption medium, Cr(III) and Cr(II) were converted to Cr(VI) using $KMnO_4$ (Snell and Snell 1959).

The amount of adsorbed Cr(VI) ions per unit biosorbent (milligrams of metal ions per gram of dry biosorbent) was obtained using the following expression:

$$q = [(C_o - C)\ V]/m \quad (1)$$

where q is the amount of Cr(VI) adsorbed onto the unit amount of the biosorbent (mg/g); C_o and C are the concentrations of the Cr(VI) ions in the initial solution (mg/L) before and after biosorption, respectively; V is the volume of the aqueous phase (L); and m is the amount of the biomass (g).

For each set of data present, standard statistical methods were used to determine the mean values and standard deviations. To ensure the accuracy, reliability, and reproducibility of the collected data, all the batch experiments were carried out

in duplicate, and the mean values of two data sets are presented. The Cr(VI) removal efficiency for all types of adsorbents was within the range of ±2.8%. When the relative error exceeded this criterion, the data were disregarded, and a third experiment was conducted until the relative error fell within an acceptable range.

2.4 Characterization of biosorbents

FTIR spectra of the biosorbents preparations were obtained using an FTIR spectrophotometer (Mattson 1000 FTIR, UK). The dry biosorbent sample (about 0.01 g) was mixed with KBr (0.1 g) and pressed into a tablet form. The FTIR spectrum was then recorded.

The water content of all the biosorbent preparation was determined using the weights of beads before and after uptake of water.

The surface morphology of the *P. boryanum* biomass immobilized alginate and alginate–gelatin beads was examined using scanning electron microscopy (SEM) (JEOL, JEM 1200 EX, Tokyo, Japan).

2.5 Theoretical approach

2.5.1 Adsorption isotherms

Adsorption isotherms express the relationship between the amount of adsorbed metal ions per unit mass of biosorbent (q_{eq}) and the metal concentration in solution (C_{eq}) at equilibrium. The Langmuir adsorption model is based on the assumption of surface homogeneity such as equally available adsorption sites, monolayer surface coverage, and no interaction between adsorbed species (Langmuir 1918). The mathematical description of this model is as follows:

$$q_{eq} = q_m b\, C_{eq} / \left(1 + b\ C_{eq}\right) \tag{2}$$

where C_{eq} and q_{eq} also show the residual metal concentration and the amount of metal adsorbed on the biosorbents at equilibrium, respectively, and b (b is equal to K_a, and it is the dependency of the equilibrium association constant) is the energy of sorption or sorption equilibrium constant (L/mg) of the system. The maximum adsorption capacity, q_m, is the solid-phase concentration corresponding to a condition in which all available sites are filled.

The essential characteristics of a Langmuir isotherm can be expressed in terms of a dimensionless constant separation factor called the equilibrium parameter, R_L, which is used to predict if an adsorption system is "favorable" or "unfavorable." It is by the following relationship:

$$R_L = 1/1 + bC_o \tag{3}$$

where C_o is the initial Cr(VI) concentration. The value of R_L indicates the shape of isotherm to be either unfavorable ($R_L > 1$) or linear ($R_L = 1$) or favorable ($0 < R_L < 1$) or irreversible ($R_L = 0$).

The Freundlich equation is the empirical relationship whereby it is assumed that the adsorption energy of Cr(VI) binding to a site on a biosorbent depends on whether or not the adjacent sites are already occupied (Freundlich 1906). One limitation of the Freundlich model is that the amount of adsorbed solute increases indefinitely with the concentration of solute in the solution. This empirical equation takes the form:

$$q_{eq} = K_F \left(C_{eq}\right)^{1/n} \tag{4}$$

where K_F and n are the Freundlich constants, the characteristics of the system. K_F and n are the indicators of the adsorption capacity and adsorption intensity, respectively.

2.5.2 Biosorption kinetic modeling

In order to examine the controlling mechanism of biosorption process such as mass transfer and chemical reaction, kinetic models were used to test experimental data. The kinetic models (pseudo-first- and second-order equations) can be used in this case assuming that the measured concentrations are equal to adsorptive sites concentrations on the cell surface. The first-order rate equation of Lagergren is one of the most widely used for the sorption of solute from a liquid solution (Lagergren 1898). It may be represented as follows:

$$\log\left(q_{eq} - q_t\right) = \log q_{eq} - \left(k_1 \cdot t\right)/2.303 \tag{5}$$

where q_{eq} is the experimental amount of Cr(VI) biosorbed at equilibrium (mg/g), q_t is the the amount of Cr(VI) biosorbed at time t (mg/g), and k_1 is the equilibrium rate constant of first-order adsorption (min^{-1}). A plot of $\log(q_{eq}-q_t)$ against t should give a straight line to confirm the applicability of the kinetic model. In a true first-order process $\log q_{eq}$ should be equal to the intercept of a plot of $\log(q_{eq}-q_t)$ against t.

Ritchie proposed a second-order rate equation for the kinetic adsorption of gases on solids (Ritchie 1977). The Ritchie's second-order equation based on biosorption equilibrium capacity is expressed in the form:

$$\left(1/q_t\right) = \left(1/k_2 q_{eq} t\right) + \left(1/q_{eq}\right) \tag{6}$$

where k_2 (g/mg min) is the rate constant of the second-order adsorption. From Eq. 6, a plot of $1/q_t$ versus $1/t$ should give a straight line to confirm for the applicability of the second-order kinetic model. The rate constant (k_2) and adsorption at equilibrium (q_{eq}) can be obtained from the intercept and slope, respectively, and there is no need to know any parameter beforehand.

3 Results and discussion

3.1 Properties of biosorbents

Biosorption of metal ions has been reported to be an alternative technology to the conventional treatment of metal-bearing effluents (Pang et al. 2011; Sun et al. 2011; Saha and Orvig 2010; Tay et al. 2011). Especially, low-cost biomaterials such as biological macromolecules and whole microbial cells (i.e., fungal, bacterial, and algal cells) have been applied with success in metal ions biosorption. Such biomass is chemically complex and contains different active groups, with properties for binding chemical substances or ions, after attracting them from solution (Deng et al. 2009).

Alginate, alginate–gelatin, alginate–cells, and alginate–gelatin–cell beads were prepared by ionic cross-linking with divalent calcium ions. The Na alginate fractions of the formulations were precipitated in bead form in the calcium chloride solution. The gelatin containing preparation was additionally cross-linked with glutaraldehyde to form bridge between gelatin units. All the prepared alginate and alginate–gelatin beads with and without *P. boryanum* cells are spherical in shape with a size range of around 2.0 mm in diameter, and the morphological appearance of the bead is exemplified in Fig. 2. The surface morphologies of the alginate, alginate–cells, bare alginate–gelatin, and alginate–gelatin–cell beads are presented in Fig. 3a–d, respectively. The surface morphologies of the bare alginate–cells and alginate–gelatin–cells beads were smoother compared to the cell-free alginate and alginate–gelatin beads, respectively. As seen in Fig. 3c and d, SEM micrographs of alginate–gelatin and alginate–gelatin–cell composite beads indicate that there is no phase separation between alginate and gelatin. The difference in surface morphology between alginate and alginate–gelatin composite beads may be due to the additional glutaraldehyde cross-linking reaction for alginate–gelatin preparation. The equilibrium swelling ratios of the alginate and alginate–gelatin beads were found to be 228% and 196%, respectively. All the prepared biosorbents were stable over the experimental pH range of 2.0–8.0.

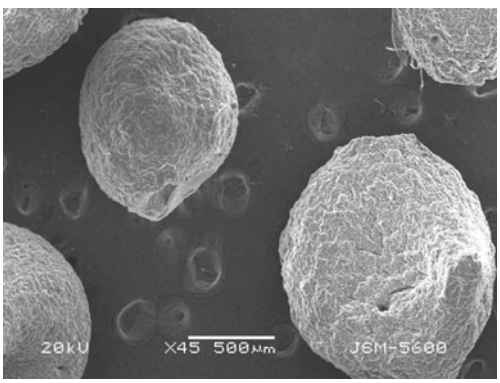

Fig. 2 Representative SEM micrograph of beads

In order to determine the functional groups responsible for Cr(VI) biosorption, FTIR spectroscopy was used. The FTIR spectra of *P. boryanum* cells, alginate–cell, alginate–gelatin–cell, and chromium (VI) loaded alginate–gelatin–cell are exemplified and presented in Fig. 4a–d, respectively. The large number and different chemical groups on the cell wall of the algal biomass (e.g., –COOH, $–NH_2$, =NH, –SH, –OH) imply that there are many types of algal cell–Cr(VI) anion interactions. The FTIR spectrum of *P. boryanum* had an intense peak at a frequency level of 3,400–3,200 cm^{-1} representing –OH stretching of carboxylic groups and also representing stretching of –NH groups (Fig. 4a). The strong peak at 1,662 cm^{-1} was caused by the bending and stretching of N–H groups of the cell wall structures of the algal biomass. The peaks at around 1,243 cm^{-1} representing C–O stretching were observed in aromatic rings. The peaks at 2,924, 2,848, 1,543, 1,381, and 1,053 cm^{-1} representing C–H stretching vibrations, N–H bending (scissoring), $–CH_3$ wagging (umbrella deformation), and C–OH stretching vibrations, respectively, were due to the several functional groups present on the algal cell walls. It should be noted that the peaks of N–H stretching vibration at 1,053 cm^{-1} were also masked with the broad band of C–O stretching vibration. In addition, there was a band at 540–470 cm^{-1} representing C–N–C scissoring was found in polypeptide structure of the algal cell wall components. The FTIR spectrum of alginate–cell composition is shown in Fig. 4b. These spectra provide clear evidences of presence of algal cell in the composite beads. After immobilization of algal biomass in alginate gel, a new peak appeared at 2,243 cm^{-1} is due to stretching vibration of $–NH_2^+$ as well as $–NH_3^+$ (Benning et al. 2004). Another new peak also appeared at 1,743 cm^{-1}, which is a characteristic of the C=O stretching vibrations, which indicates the increase in the intensity of carbonyl groups after immobilization of algal cell in alginate (Fig. 4b). In addition, the peak at 824 cm^{-1} can be attributed to the glycoside linkage in the polysaccharide structure of the composite beads. The peak at 533 cm^{-1} representing O–C–O scissoring and C=O bending vibrations was due to lipids. The FTIR spectrum of alginate–gelatin–cell composition is presented in Fig. 4c; the alginate–gelatin–cell components had a peak at 3,429 cm^{-1} representing –OH stretching of carboxylic groups. The strong peak at 1,650 cm^{-1} was caused by the bending and stretching of N–H groups of both the cell wall structures of the algal biomass and gelatin. FTIR study was also carried out to understand the type of functional groups responsible for Cr(VI) binding process with the alginate–gelatin–cell composition (Fig. 4d). There is a considerable change in the spectrum after the biosorption of Cr (VI). As seen in Fig. 4d, the presence of new peaks at 1,638, 924, 733, and 638 cm^{-1} in the Cr(VI) loaded alginate–gelatin–

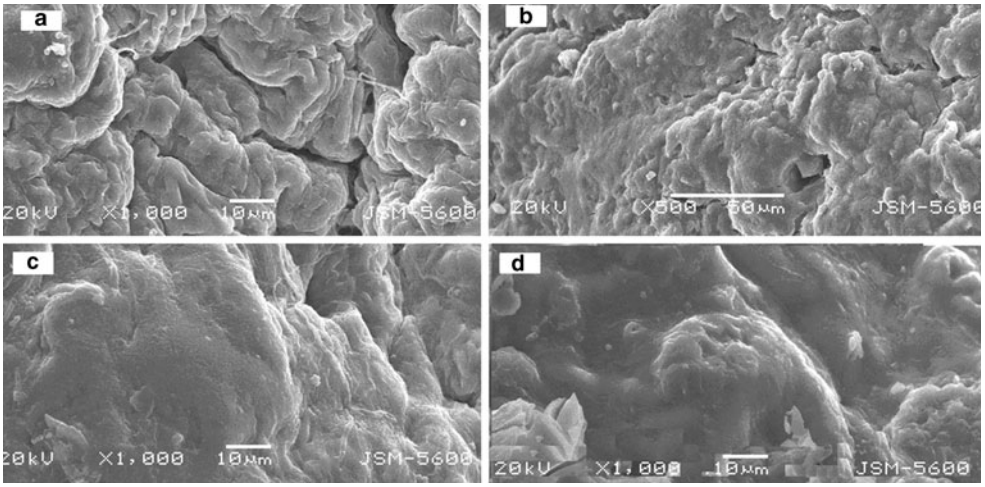

Fig. 3 SEM micrograph of the surface morphologies of alginate, alginate–cell, alginate–gelatin, and alginate–gelatin–cell beads

cell composition. In the FTIR spectra of the Cr(VI) loaded composite beads, the new band is observed at 1,638 cm^{-1} and can be assigned as stretching vibration of aromatic groups after biosorption of Cr(VI) anions. The peak at 924 cm^{-1} is attributed to the stretching vibration of Cr=O in $HCrO_4^-$ and the presence of Cr(VI)–O bond. This indicates that the nitrogen of the amine is protonated and forms an ion pair with $HCrO_4^-$ in the acidic medium (Holman 2002). The peaks at 733 and 638 cm^{-1} confirmed the formation of Cr(VI) complex. Finally, the result indicated that the chemical interactions such as ion exchange between the hydrogen atoms of carboxyl (–COOH), hydroxyl (–OH), and amine ($–NH_2$) group of biomass and metal ions are mainly involved in biosorption of Cr(VI) onto alginate–gelatin–cell bead surface.

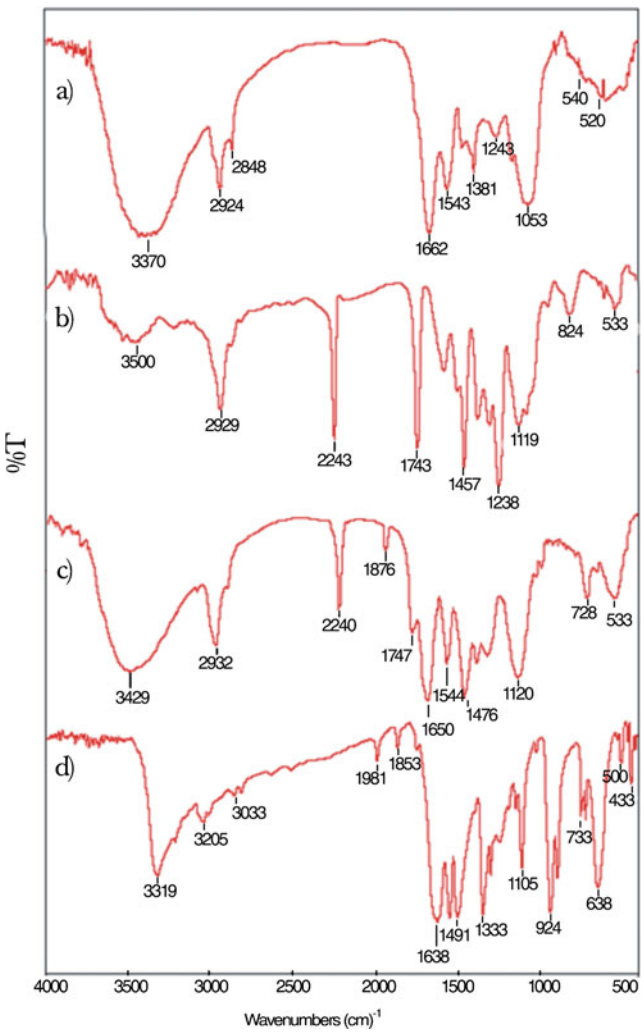

Fig. 4 FTIR spectra: **a** *P. boryanum* cells; **b** alginate–cell; **c** alginate–gelatin–cell; **d** chromium (VI) loaded alginate–gelatin–cell

3.2 Effect of pH on the biosorption capacity of the biosorbents

Removal of Cr(VI) anions by differently formulated composite biosorbents has been found to vary as a function of pH of the solution. The Cr(VI) biosorption depends on protonation or unprotonation of various functional groups on the surface of all the tested biosorbents. There was maximum adsorption of Cr(VI) on the tested biosorbents at pH 2.0, but above this, Cr(VI) removal declined. At pH 2.0, protonation of amino groups on the free *P. boryanum* biomass and immobilized counterpart in the alginate and alginate–gelatin increase the net positive charge and enhances the biosorption of negatively charged Cr(VI) anions by electrostatic binding (Bayramoglu and Arica 2009; Guerra et al. 2010; Deng et al. 2009). The protonation of certain functional groups of the tested biosorbents and the presence of hydronium ions around the binding sites can cause an enhanced attraction of chromium ions to biosorbents surface at this acidic pH. As the solution pH increases, the surface of the biosorbents becomes negatively charged due to functional groups, which repulse negatively charged chromate ions ($HCrO_4^-$, $Cr_2O_7^{2-}$, and $Cr_4O_{13}^{2-}$). The involvement of amino group in the biosorption of Cr(VI) ions also confirmed these biosorbents by the FTIR analysis as presented above. However, beyond the p*K*a value of carboxyl groups (around pH 5.0), the net charge on algal cells, gelatin,

and alginate becomes negative, and at the same time, the solution also contains CrO_4^{2-} ions only. The distribution of Cr(VI) ions species is dependent on both the total concentration of Cr(VI) and the pH of the biosorption medium. As the pH increased, the overall surface charge on the cell walls became negative, and biosorption decreased. As seen in Fig. 5, the adsorptions of Cr(VI) anions on the alginate, alginate–gelatin, free *P. boryanum* biomass, alginate–cells, and alginate–gelatin–cells were found to be 20%, 47%, 52%, 73% and 97%, respectively, at pH 2.0. Thus, a maximum Cr(VI) removal was observed with the alginate–gelatin–cell biosorbents. The observed increase in the removal efficiency of this biosorbent is due to the incorporation of gelatin and algal cells in the alginate. Thus, the number of active sites on biosorbent formulation increases, and consequently, the percent removal of Cr(VI) increases. Finally, the removal efficiency of all the tested biosorbents remained at a low level through the tested pH range; all subsequent biosorption experiments were conducted at pH 2, the optimum pH for adsorption of Cr(VI) ions on the tested biosorbents.

3.3 Effect of contact time

Figure 6 shows the comparative data of the effect of contact time on the extent of biosorption of Cr(VI) on all the tested biosorbents at 100 mg/L initial Cr(VI) concentration. As seen in this figure, the biosorption of Cr(VI) on free algal cells, alginate, alginate–gelatin, alginate–cells, and alginate–gelatin–cell beads is quick and, after 90 min, the complete biosorption equilibrium. The amount of Cr(VI) ion removal efficiency reached a maximum of 52%, 20%, 47%, 73%, and 97%, for the free algal cells, alginate, alginate–gelatin, alginate–cells, and alginate–gelatin–cells, respectively.

3.4 Effect of adsorbent dosage on the biosorption capacity

The influence of adsorbent dosage on Cr(VI) biosorption was studied by varying the amount of the biosorbent from 0.025 to 0.20 g in each adsorption medium. Figure 7 shows that the percentage removal of Cr(VI) anions increased for the free algal cells from 21% to 52%, for alginate–cells from 41% to 73%, and for alginate–gelatin–cells from 63% to 97%, with an increase in adsorbent dosage from 0.025 to 0.20 g in 25 mL adsorption medium containing 100 mg/L Cr (VI). This trend is obvious because, as the adsorbent dose increases, the number of active sites available in the adsorption medium also increases, which makes the greater availability of the functional binding sites for Cr(VI) biosorption (Mohan et al. 2005).

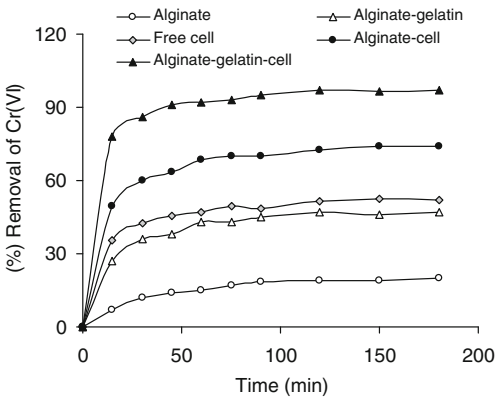

Fig. 6 Biosorption rates of Cr(VI) on *P. Boryanum* cell, alginate, alginate–gelatin, alginate–cell, and alginate–gelatin–cell beads: biosorption conditions, initial concentration of Cr(VI) anions, 100 mg/L; pH 2.0; temperature, 25°C

3.5 Experimental biosorption isotherms

Figure 8 shows the biosorption of Cr(VI) onto all of the tested biosorbents with various initial Cr(VI) concentrations. At a lower concentration, all the Cr(VI) ions in the solution would react with the binding sites and thus facilitated almost complete adsorption. At a higher concentration, more Cr(VI) ions are left unsorbed in the solution due to the saturation of the binding sites. This indicates that the energetically less favorable sites

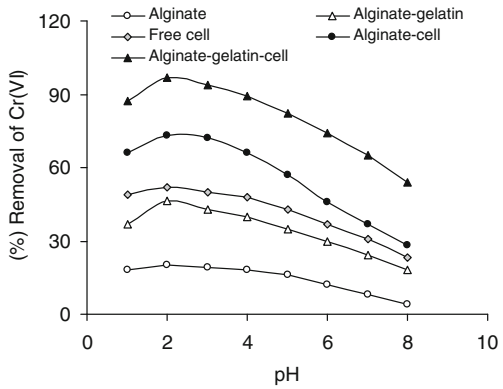

Fig. 5 Effect of pH on Cr(VI) biosorption. Biosorption conditions: initial concentration of metal ions, 100 mg/L; temperature, 25°C

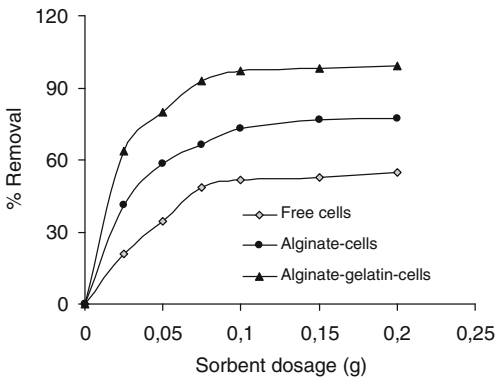

Fig. 7 Effect of biosorption dosage on Cr(VI) removal efficiency of the biosorbents

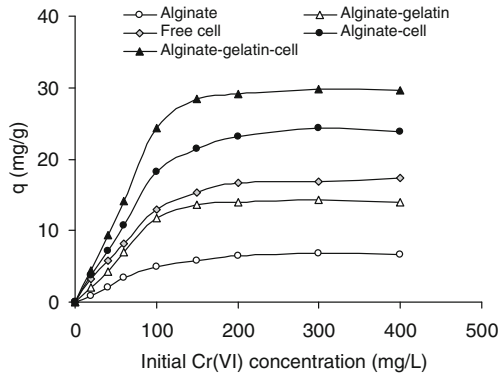

Fig. 8 Biosorption capacities of the *P. Boryanum* cells, alginate, alginate–gelatin, alginate–cell, and alginate–gelatin–cell beads: for different concentrations of Cr(VI) ions, biosorption conditions, pH 2.0, temperature of 25°C

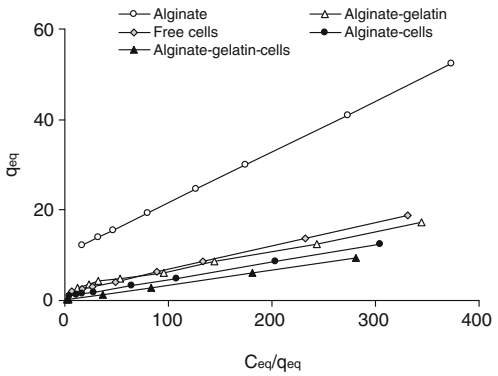

Fig. 9 Langmuir isotherm model plots for the biosorption of Cr(VI) on the *P. Boryanum* cells, alginate, alginate–gelatin, alginate–cell, and alginate–gelatin–cell beads

become involved with increasing Cr(VI) ion concentration in aqueous solutions (Sun et al. 2011). The biosorption values increase with increasing concentration of Cr(VI) ions, and a saturation value is achieved at Cr(VI) anion concentration of 150 mg/L, which represents saturation of the active binding sites on all the tested biosorbents (Fig. 8). In the case of high Cr (VI) concentration, mass transfer limitations were also overcome by high driving force, which was the concentration difference of Cr(VI) between the liquid and the solid phases. The maximum Cr(VI) biosorption capacities in the studied Cr (VI) concentration range were 17.3, 6.7, 14.0, 23.8, and 29.6 mg/g for the free algal cells, alginate, alginate–gelatin, alginate–cells, alginate–gelatin–cells, respectively, which correspond to an initial Cr(VI) concentration of 400 mg/L.

3.6 Adsorption isotherms models

The experimental biosorption isotherm was studied by varying the concentration of Cr(VI) solutions with a fixed dose of sorbent. Equilibrium data were well plotted by Langmuir models (Fig. 9). The Langmuir and Freundlich sorption constants calculated from the corresponding isotherms with the correlation coefficients are presented in Table 1. Comparing the correlation coefficients listed in Table 1, we can draw a conclusion that the biosorption of Cr(VI) metal ions onto five kinds of biosorbents well followed as Langmuir isotherm equation under the used concentration range.

To predict the theoretical maximum biosorption capacity of the alginate–cells and alginate–gelatin–cells beads, Langmuir isotherm was used to fit the experimental data, and the corresponding equations are also shown in Fig. 9. The Langmuir constant (b) increased from 1.09×10^{-2} to 4.85×10^{-2} L/mg and from 2.12×10^{-2} and 21.3×10^{-2} L/mg for the biosorbents when algal cell was entrapped into alginate and alginate–gelatin beads, respectively, indicating the stronger affinity of these biosorbents for Cr(VI) anions compared with the free algal cells, alginate beads, and alginate–gelatin beads. Langmuir constant q_m also indicates that the biosorption capacity of biosorbent increases with the following order: alginate–gelatin–cells> alginate–cells> free algal cells> alginate–gelatin>alginate.

A further analysis of the Langmuir equation can be made on the basis of a dimensionless equilibrium parameter, R_L, also known as the separation factor, given by Eq. 3. Based on the effect of separation factor, R_L values are in the range of $0<R_L<1$, which indicates that the sorbents are favorable biosorbents for Cr(VI) removal from aqueous solution (Table 1).

3.7 Kinetic studies

To elucidate the biosorption mechanism, the first- and second-order kinetic models were tested to fit the experimental data obtained from batch Cr(VI) anion removal experiments. The first- and second-order equation parameters together with correlation coefficients are listed in Table 2. The data illustrated good compliance with the pseudo-second-order rate law based on sorption capacity because the coefficients of determination were higher than 0.994 for all the tested biosorbents systems in this study (Table 2). The correlation coefficients for the pseudo-first-order equation obtained at all the tested biosorbents were low. The biosorption data are better fitted by the second-order kinetic model as compared to the first-order kinetic model. Figure 10 shows a plot of $1/q_t$ versus t for biosorption of Cr(VI) for the second-order equation. The straight lines in plot of linear second-order equation show good agreement of experimental data with the second-order kinetics equation for the free algal cells and alginate, alginate–gelatin, alginate–cells, and alginate–gelatin–cell beads. The pseudo-second-order model is based on the assumption that the rate limiting step is a chemical sorption involving valance forces through the sharing or exchange of electrons between

Table 1 The isotherm models constants and correlation coefficients and R_L values based on Langmuir equation for biosorption of Cr(VI) on *P. Boryanum* cells and alginate, alginate–gelatin, alginate–cells, and alginate–gelatin–cell beads

Biosorbent	Langmuir				Freundlich			
	$q_{m(exp)}$ (mg/g)	q_m (mg/g)	b ($\times 10^2$ L/mg)	R^2	n	K_F	R^2	R_L[a]
Alginate	6.73	8.90	1.09	0.980	1.61	0.24	0.926	0.1866
Alginate–gelatin	14.0	16.7	2.12	0.982	1.85	0.86	0.890	0.1055
Free algal cells	17.3	19.2	3.24	0.998	2.56	2.41	0.917	0.0716
Alginate–cells	23.8	26.0	4.85	0.997	2.32	2.78	0.911	0.0490
Alginate–gelatin–cells	29.6	30.4	21.3	0.999	3.94	8.69	0.754	0.0116

[a] R_L value calculated at 400 mg/L initial Cr(VI) concentration

the sorbents and adsorbate. It provides the best correlation of the data (Mohan et al. 2005).

3.8 Evaluation of thermodynamic parameters for biosorption of Cr(VI)

In order to evaluate the feasibility and the effect of temperature better, for Cr(VI) biosorption on the free algal cells, alginate–cells, and alginate–gelatin–cell thermodynamic parameters such as activation energy (E_a), standard free energy change ($\Delta G°$), standard enthalpy change ($\Delta H°$), and standard entropy change ($\Delta S°$) were also obtained. Batch adsorption runs of Cr (V) on biosorbents were performed at different temperatures (15°C, 25°C, 35°C, and 45°C), and the results are summarized in Table 3. The biosorption capacities of the tested biosorbents were increased by increasing temperatures from 15°C to 45°C. This may be due to an increase in thermal energy of the adsorbing species, which leads to higher adsorption capacity. R_L at different temperatures were found to be >0 and <1, indicating the favorable aqueous media in differently formulated biosorbents (data not shown). Activation energy is determined according to the pseudo-second-order rate constant and is expressed as a function of temperature by the Arhenius equation, $k=A_o \exp(-E_a/RT)$. A_o is the temperature independent factor. The value of k is obtained from the second-order kinetic model equation and used to determine the activation energy of biosorption (E_a). The value of the activation energy, E_a, can be determined from the slope of ln$k$ versus $1/T$ plot. The activation energies for the free algal cells and alginate, alginate–gelatin, alginate–cell, and alginate–gelatin–cell beads were calculated, and the values were found to be 7.30, 14.7, 12.5, 8.77, and 1.75 kJ/mol, respectively. The magnitude of activation energy may give an idea about the type of sorption. In physical sorption, equilibrium is usually rapidly attained and easily reversible because energy requirements are small.

The value of K_a is obtained from the Langmuir isotherm equation and used to determine the Gibbs free energy change of biosorption process ($\Delta G=-RT\ln K_a$). Standard enthalpy and entropy change values of a biosorption process can be calculated from the van't Hoff equation ($\ln K_a=\Delta S/R-\Delta H/RT$). The thermodynamic parameters for Cr(VI) biosorption by the free algal cells and alginate, alginate–gelatin, alginate–cells and alginate–gelatin–cell beads are presented in Table 3. The negative values of ΔG indicate that Cr(VI) biosorption is a spontaneous and high affinity process. When the temperature increased from 288 to 318 K, $\Delta G°$ is decreased for Cr(VI) biosorption by all the tested biosorbents. The change of Gibbs free energy decreased with increasing temperature, indicating that a better adsorption occurred at higher temperatures. The positive value of ΔH indicates the endothermic nature of biosorption. For alginate–gelatin–cell biosorbent, the biosorption enthalpy change is larger than that of alginate–gelatin

Table 2 The kinetic models constants and correlation coefficients for the biosorption of Cr(VI) on the *P. Boryanum* cells and alginate, alginate–gelatin, alginate–cells, and alginate–gelatin–cell beads

Biosorbent		First order			Second order		
	$q_{m(exp)}$ (mg/g)	q_{eq} (mg/g)	k_1 ($\times 10^2$ min^{-1})	R^2	q_{eq} (mg/g)	k_2 ($\times 10^2$ g/mg min)	R^2
Alginate	6.73	13.8	4.61	0.931	8.61	2.76	0.998
Alginate–gelatin	14.0	7.26	2.53	0.974	15.2	7.48	0.997
Free algal cells	17.3	11.5	3.39	0.956	18.5	9.28	0.995
Alginate–cells	23.8	10.6	2.94	0.977	24.9	12.2	0.996
Alginate–gelatin–cells	29.6	17.1	4.55	0.926	30.2	24.0	0.994

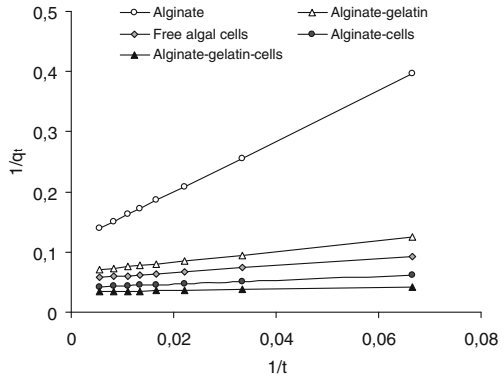

Fig. 10 The second-order plots for the biosorption of Cr(VI) on the *P. Boryanum* cell, alginate, alginate–gelatin, alginate–cell, and alginate–gelatin–cell beads

(Table 3). It means that the interaction between Cr(VI) and the alginate–gelatin–cell surface is stronger and leads to an enhanced biosorption. Positive ΔS values for Cr(VI) biosorption were found for the free algal cells and alginate–cells and alginate–gelatin–cells, suggesting an increase on randomness at the solid–solution interface during biosorption and/or some structural alterations in the biosorbents during the Cr(VI) binding. As the free energy changes are negative and accompanied by positive entropy changes, the adsorption reactions are spontaneous with a high affinity (Bayramoglu et al. 2009a; Bayramoglu et al. 2009b).

4 Conclusions

Biosorption of Cr(VI) from aqueous solutions using the free algal cells and immobilized forms in alginate and alginate–gelatin biosorbents was investigated as a function of pH, contact time, initial Cr(VI) concentration, and temperature through batch experiments. The analysis of the FTIR spectra showed the presence of functional groups (i.e., carboxyl, primary and secondary amino groups, and hydroxyl groups) able to interact with protons or Cr(VI) anions. Equilibrium time was found to set in around 90 min, with reduction in chromium levels up to 97%. The kinetics, adsorption isotherms, and thermodynamic parameters were examined. The equilibrium isotherms obtained were close to the Langmuir isotherm, which showed that the adsorbent surface contained adsorption sites suitable for the operation of the monolayer adsorption. Biosorption of Cr(VI) on the tested biosorbents follows the second-order kinetic model under the given experimental conditions. The positive values of both ΔH and ΔS suggest an

Table 3 The isotherm models constants and correlation coefficients based on Langmuir equation for biosorption of Cr(VI) on the all the tested biosorbents and thermodynamic parameters and sorption energies

Biosorbents	T (K)	Langmuir parameters				Thermodynamic parameters			
		$q_{m(exp)}$ (mg/g)	q_m (mg/g)	b ($\times 10^2$ L/mg)	R^2	ΔG (kJ/mol)	ΔH (kJ/mol)	ΔS (kJ/mol K)	E_a (kJ/mol)
Alginate	288	5.41	6.94	0.99	0.989	1.60			
	298	6.73	8.90	1.09	0.980	1.41			
	308	8.92	10.5	1.86	0.994	0.08	39.0	0.128	14.7
	318	9.78	11.2	2.49	0.996	-0.68			
Alginate–gelatin	288	13.2	15.6	2.05	0.991	-0.16			
	298	14.0	16.7	2.12	0.982	-0.24			
	308	15.6	17.9	2.56	0.990	-0.73	19.7	0.068	12.5
	318	17.8	19.1	4.64	0.994	-2.33			
Free algal–cell	288	15.1	17.5	2.13	0.995	-0.25			
	298	17.3	19.2	3.24	0.998	-1.29			
	308	18.6	20.2	3.85	0.997	-1.78	18.1	0.064	7.30
	318	20.4	21.7	4.47	0.999	-2.23			
Alginate–cells	288	19.8	22.3	3.44	0.993	-1.39			
	298	23.8	26.0	4.85	0.997	-2.29			
	308	27.9	26.4	5.96	0.999	-2.90	25.2	0.093	8.77
	318	26.2	27.5	9.13	0.998	-4.12			
Alginate–gelatin–cells	288	22.7	23.8	8.40	0.998	-14.6			
	298	29.6	30.4	21.3	0.999	-17.4			
	308	34.9	35.5	27.4	0.998	-18.6	44.5	0.251	1.75
	318	37.8	38.3	53.7	0.999	-20.9			

endothermic reaction, increasing in randomness at the solid–liquid interface during the biosorption process under studied conditions. Finally, alginate–gelatin–cell biosorbent can be used as an effective removal of Cr(VI) ions from aqueous media.

References

Akar T, Tunali S (2006) Biosorption characteristics of *Aspergillus flavus* biomass for removal of Pb(II) and Cu(II) ions from an aqueous solution. Bioresour Technol 97:1780–1787

Akar T, Kaynak Z, Ulusoy S, Yuvaci D, Ozsari G, Tunali-Akar S (2009) Enhanced biosorption of nickel(II) ions by silica-gel-immobilized waste biomass: biosorption characteristics in batch and dynamic flow mode. J Hazard Mater 163:1134–1141

Arica MY, Bayramoglu G, Yilmaz M, Bektas S, Genc O (2004) Biosorption of Hg^{2+}, Cd^{2+}, and Zn^{2+} by Ca-alginate and immobilized wood-rotting fungus *Funalia trogii*. J Hazard Mater 109:191–199

Arica MY, Yalcin E, Ince O, Bayramoglu G (2005) Utilisation of native, heat and acid-treated microalgae *Chlamydomonas reinhardtii* preparations for biosorption of Cr(VI) ions. Process Biochem 40:2351–2358

Bajpai J, Shrivastava R, Bajpai AK (2004) Dynamic and equilibrium studies on adsorption of Cr(VI) ions onto binary bio-polymeric beads of cross linked alginate and gelatin. Colloid Surface A 236:83–92

Bayramoglu G, Arica MY (2008) Removal of heavy mercury(II), cadmium(II) and zinc(II) metal ions by live and heat inactivated *Lentinus edodes* pellets. Chem Eng J 143:133–140

Bayramoglu G, Arica MY (2009) Construction a hybrid biosorbent using *Scenedesmus quadricauda* and Ca-alginate for biosorption of Cu(II), Zn(II) and Ni(II): Kinetics and equilibrium studies. Bioresour Technol 100:186–193

Bayramoglu G, Celik G, Arica MY (2006) Studies on accumulation of uranium by fungus *Lentinus sajor-caju*. J Hazard Mater 136:345–353

Bayramoglu G, Altintas B, Arica MY (2009a) Adsorption kinetics and thermodynamic parameters of cationic dyes from aqueous solutions by using a new strong cation exchange resin. Chem Eng J 152:339–346

Bayramoglu G, Gursel I, Tunalı Y, Arica MY (2009b) Biosorption of phenol and 2-chlorophenol by *Funalia trogii* pellets. Bioresour Technol 100:2685–2691

Benning LG, Phoenix VR, Yee N, Tobin MJ (2004) Molecular characterization of cyanobacterial silicification using synchrotron infrared micro-spectroscopy. Geochim Cosmochim Acta 68:729–741

Cristani M, Naccari C, Nostro A, Pizzimenti A, Trombetta D, Pizzimenti F (2011) Possible use of *Serratia marcescens* in toxic metal biosorption (removal). Environ Sci Pollut Res 19:161–181. doi:10.1007/s11356-011-0539-8

Deng L, Zhang Y, Qin J, Wang X, Zhu X (2009) Biosorption of Cr(VI) from aqueous solutions by nonliving green algae *Cladophora albida*. Minerals Eng 22:372–377

Freundlich H (1906) Adsorption in solution. Z Phys Chem 40:1361–1368

Gadd GM (1993) Interaction of fungi with toxic metals. New Phytol 124:25–60

Genc O, Soysal L, Bayramoglu B, Arica MY, Bektas S (2003) Procion Green H-4G immobilized poly(hydroxyethylmethacrylate/chitosan) composite membranes for heavy metal removal. J Hazard Mater 97:111–125

Guerra DL, Oliveira HCP, da Costa PCC, Viana RR, Airoldi C (2010) Adsorption of chromium(VI) ions on Brazilian smectite: effect of contact time, pH, concentration, and calorimetric investigation. Catena 82:35–44

Holman HYN (2002) Real time characterization of biogeochemical reduction of Cr(VI) on basalt surfaces by SR-FTIR imaging. Geomicrobiol J 16:307–324

Khani MH (2011) Statistical analysis and isotherm study of uranium biosorption by *Padina* sp. algae biomass. Environ Sci Pollut Res 18:790–799

Kuyucak N, Volesky B (1990) Biosorption by algal biomass. In: Volesky B (ed) Biosorption of heavy metals. CRC, Boca Raton, pp 173–198

Lagergren S (1898) Zur theorie der sogenannten adsorption geloster stoffe. Kungliga Svenska Vetenskapsakademiens Handlingar 24:1–39

Langmuir I (1918) The adsorption of gases on plane surfaces of glass, mica and platinum. J Am Chem Soc 40:1361–1403

Mohan D, Singh KP, Singh VK (2005) Removal of hexavalent chromium from aqueous solution using low-cost activated carbons derived from agricultural waste materials and activated carbon fabric cloth. Ind Eng Chem Res 44:1027–1042

Pang C, Liu Y-H, Cao X-H, Li M, Huang G-L, Hua R, Wang C-X, Liu Y-T, An X-F (2011) Biosorption of uranium(VI) from aqueous solution by dead fungal biomass of *Penicillium citrinum*. Chem Eng J 170:1–6

Ritchie AG (1977) Alternative to the Elovich equation for kinetics of adsorption of gases on solids. J Chem Soc Faraday Trans 73:1650–1653

Saha B, Orvig C (2010) Biosorbents for hexavalent chromium elimination from industrial and municipal effluents. Coordination Chem 254:2959–2972

Sari A, Tuzen M, Uluozlu OD, Soylak M (2007) Biosorption of Pb(II) and Ni(II) from aqueous solution by lichen (*Cladonia furcata*) biomass. Biochem Eng J 37:151–158

Silke S, Volesky B (1995) Modelling of the proton–metal ion exchange in biosorption. Environ Sci Technol 29:3049–3058

Singha B, Kumar DS (2011) Biosorption of Cr(VI) ions from aqueous solutions: kinetics, equilibrium, thermodynamics and desorption studies. Colloid Surface B 84:221–232

Snell FD, Snell CT (1959) Colorimetric methods of analysis, vol. 2, 3rd edn. Van Nostrand Company, Canada

Sun XF, Liu C, Ma Y, Wang S-G, Gao B-Y, Li X-M (2011) Enhanced Cu(II) and Cr(VI) biosorption capacity on poly(ethylenimine) grafted aerobic granular sludge. Colloid Surface B 82:456–462

Tay C, Liew HH, Yin CY, Abdul-Talib S, Surif S, Suhaimi AA, Yong SK (2011) Biosorption of cadmium ions using *Pleurotus ostreatus*: growth kinetics, isotherm study and biosorption mechanism. Korean J Chem Eng 28:825–830

Tuzen M, Uluozlu OD, Soylak M (2007) Cr(VI) and Cr(III) speciation on *Bacillus sphaericus* loaded diaion SP-850 resin. J Hazard Mater 144:549–555

Wetzel RG, Likens GE (1991) Limnological analysis, 2nd edn. Springer, New York

Yang F, Liu HJ, Qu JH, Chen JP (2011) Preparation and characterization of chitosan encapsulated *Sargassum sp*. biosorbent for nickel ions sorption. Bioresour Technol 102:2821–2828

Yipmantin A, Maldonado HJ, Ly M, Taulemesse JM, Guibal E (2011) Pb (II) and Cd(II) biosorption on *Chondracanthus chamissoi* (a red alga). J Hazard Mater 185:922–929